Supplementary Information for:

Hierarchical 3D ZnO Nanowire Structures via Fast Anodization of Zinc

D. O. Miles,[a] P. J. Cameron[b] and D. Mattia[c]

[a] Centre for Sustainable Chemical Technologies, University of Bath, Bath, UK.
[b] Department of Chemistry, University of Bath, Bath, UK.
[c] Department of Chemical Engineering, University of Bath, Bath, UK.

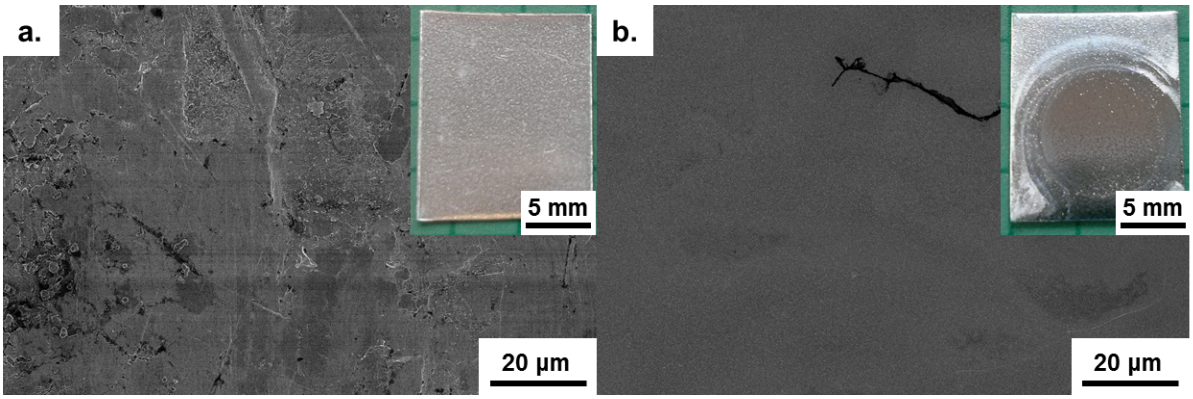

Figure S1. FESEM micrograph and photo (inset) of the zinc foil surface before (a) and after (b) the electropolishing pre-treatment. The surface can be seen to be much smoother after electropolishing. A piece of debris (black fibre) is featured (b) to ensure focus is achieved on the relatively featureless zinc surface.

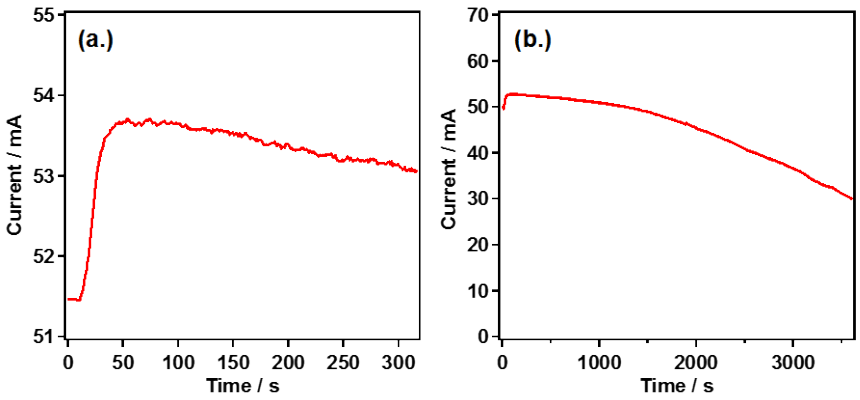

Figure S2. Current-time data recorded during anodization at constant voltage showing the initial sharp increase in current (a) followed by a slow decline in current over time (b).

Control of Nanowire Growth

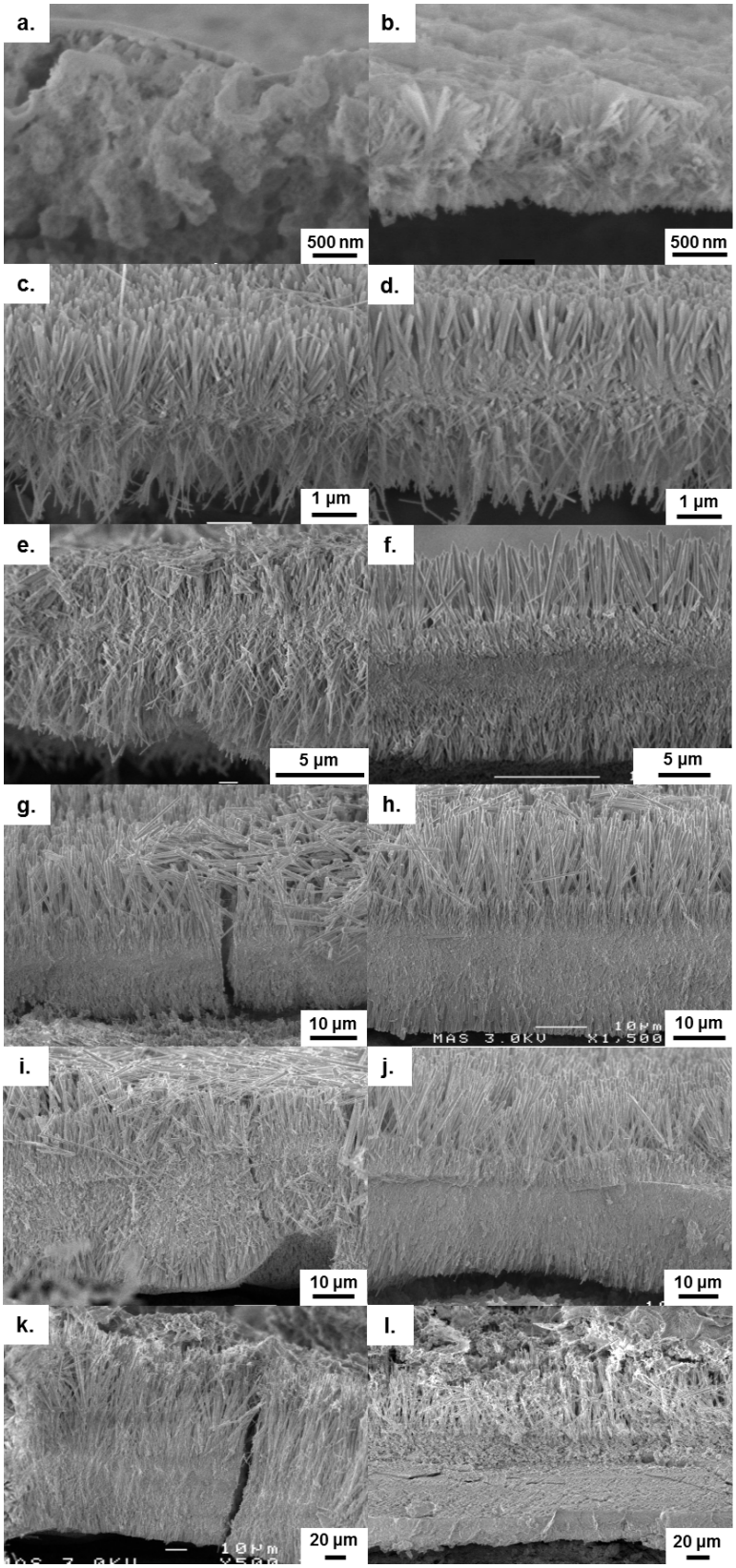

Figure S3. FESEM cross-sections of nanowire (NW) films formed after anodizations for 1 (a & b), 5 (c & d), 15 (e & f), 30 (g & h), 60 (I & j) and 120 minutes (k & l) in aqueous $NaHCO_3$ and NH_4HCO_3 electrolytes respectively.

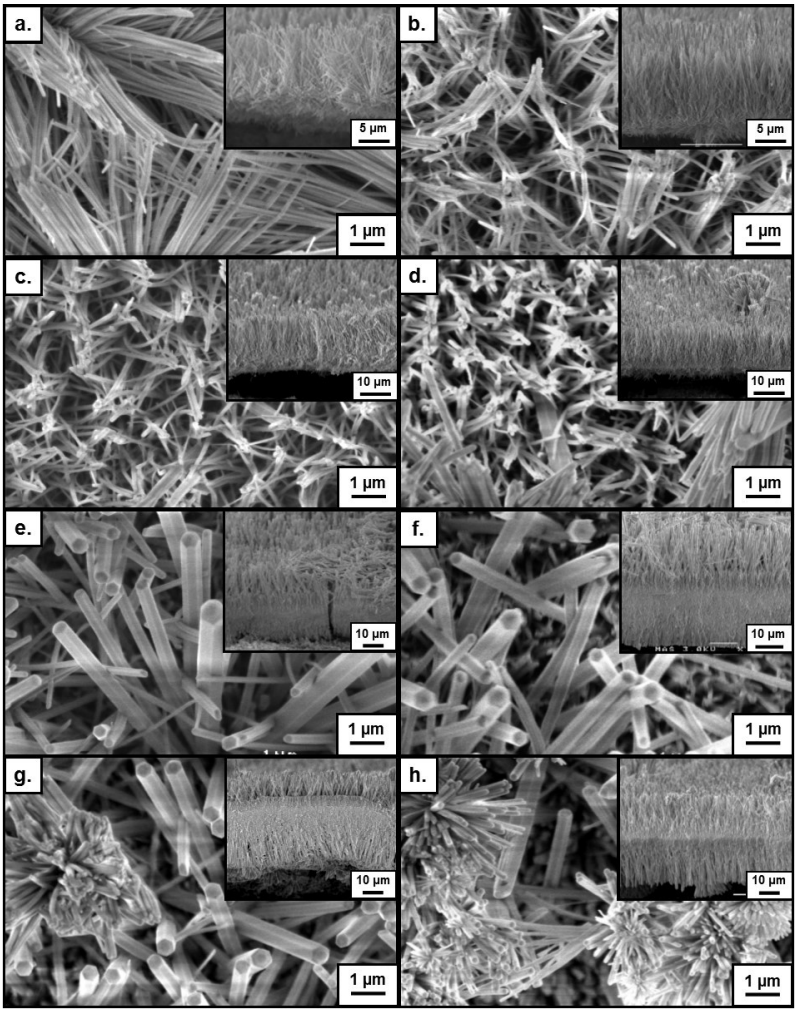

Figure S4. FESEM surface morphologies and cross-sections (inset) of nanowire arrays grown by anodization at 1 V (a & b), 2 V (c & d), 5 V (e & f) or 10 V (g & h) in electrolytes of $NaHCO_{3(aq)}$ and $NH_4HCO_{3(aq)}$ respectively.

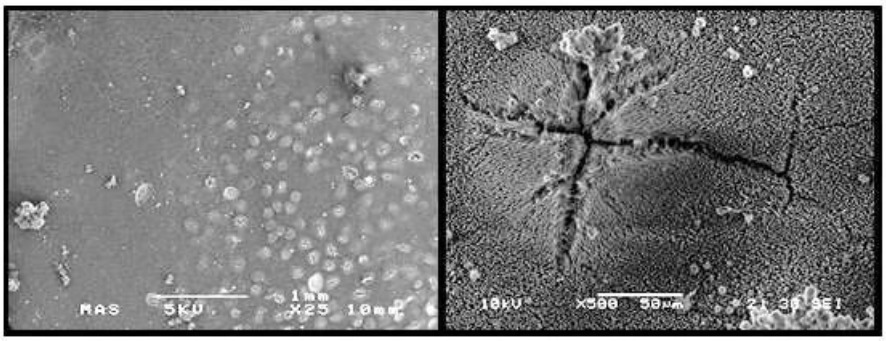

Figure S5. FESEM surface morphologies showing ruptures in the nanowire film formed at 10 V. The rupture is likely due to oxygen gas formation underneath the nanowire film.

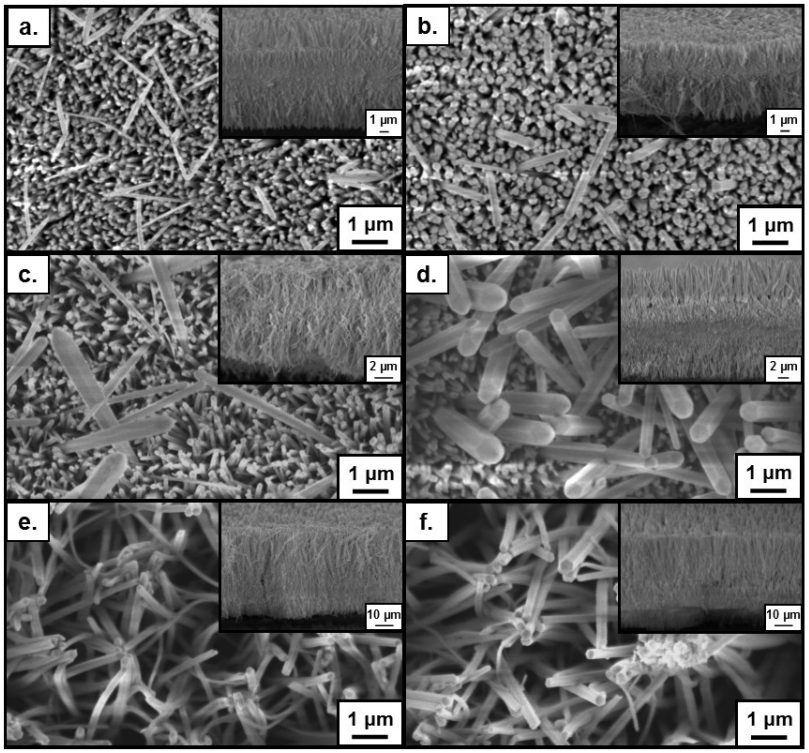

Figure S6. FESEM surface morphologies and cross-sections (inset) of nanowire arrays grown by anodization at temperatures of 5 (a & b), 10 (c & d) or 20 °C (e & f) for electrolytes of $NaHCO_{3(aq)}$ and $NH_4HCO_{3(aq)}$ respectively.

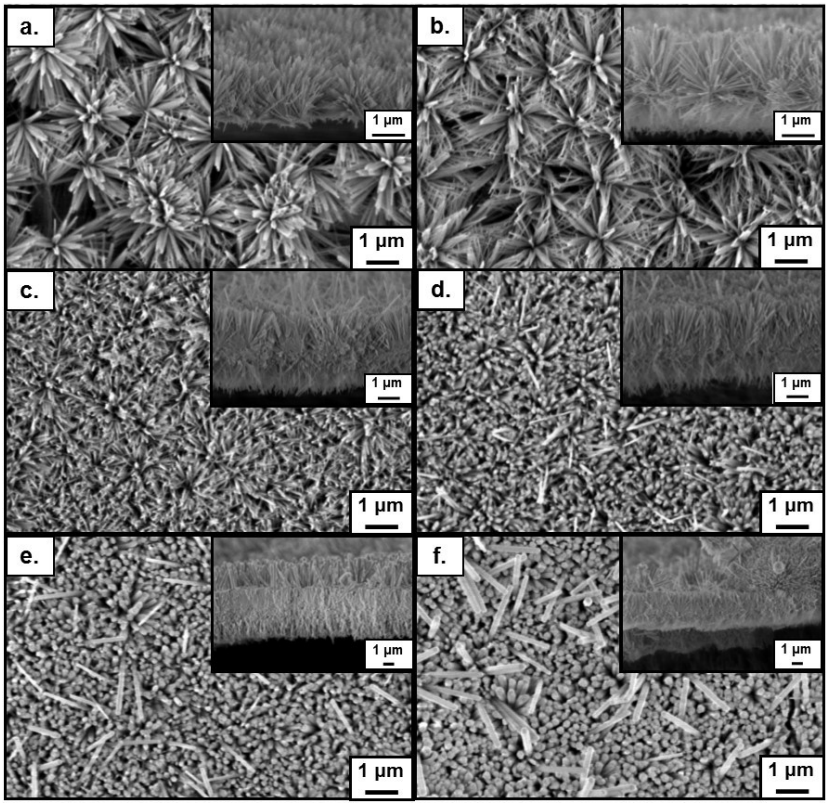

Figure S7. FESEM surface morphologies and cross-sections (inset) of nanowire arrays grown by anodization at electrolyte concentrations of 50 (a & b), 100 (c & d) or 200 mM (e & f) for electrolytes of $NaHCO_{3(aq)}$ and $NH_4HCO_{3(aq)}$ respectively.

Rationalising the Rapid Nanowire Growth

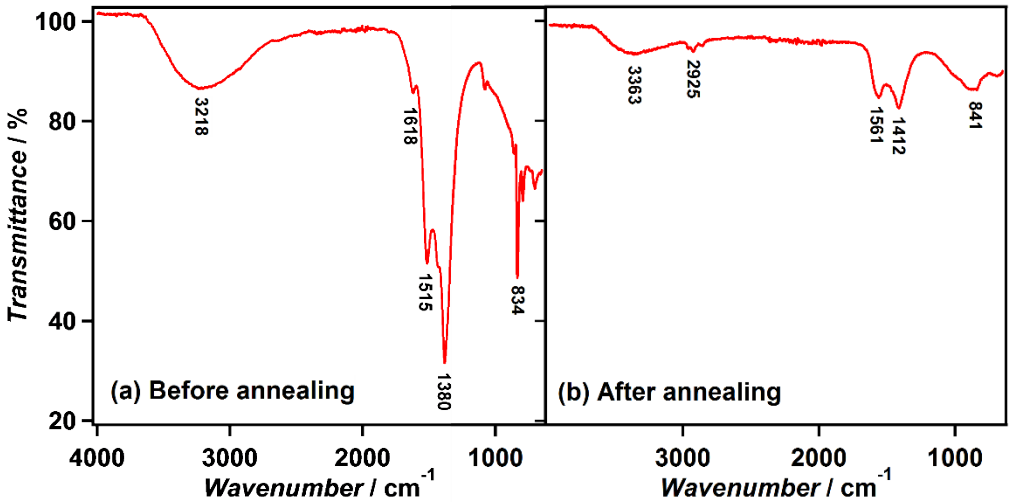

Figure S8. FT-IR spectrum of the nanowire film prepared by anodization (a) and after annealing at 300 °C for 1 h (b).

Conversion to ZnO

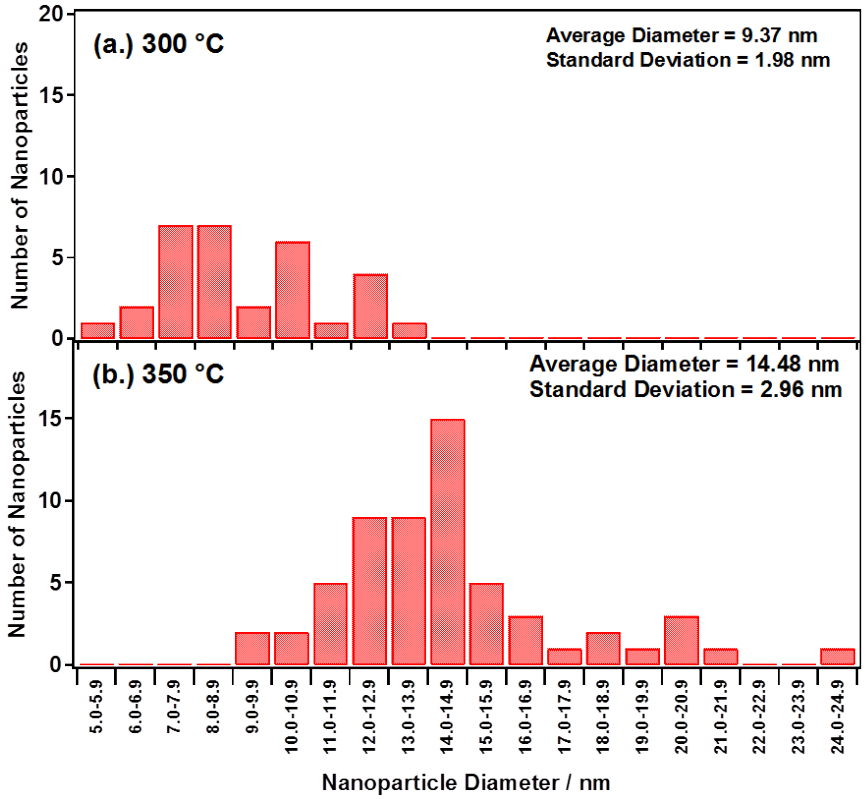

Figure S9. Particle size distributions determined from TEM for polycrystalline nanowires formed after annealing at 300 °C (a) and 350 °C (b).

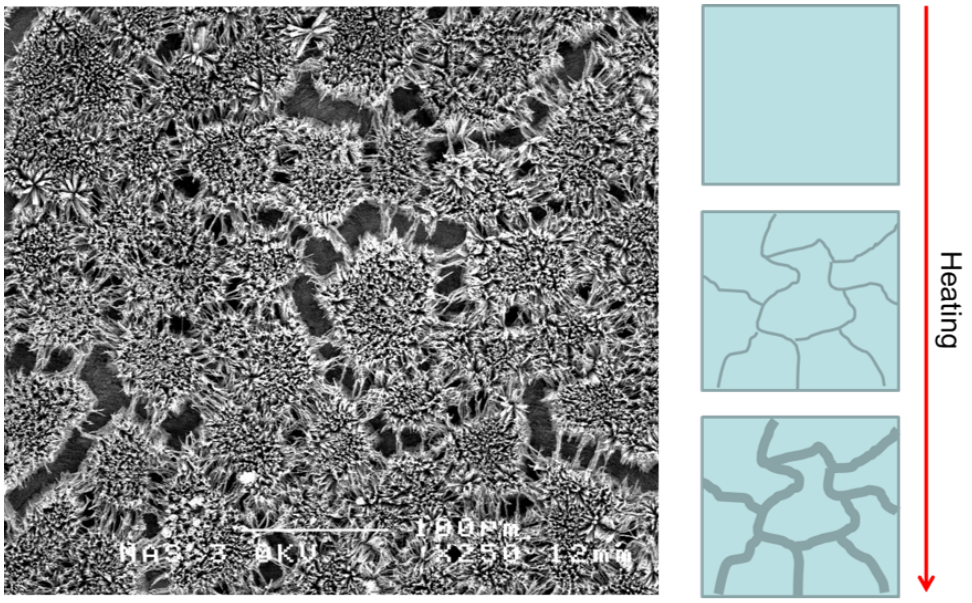

Figure S10. FESEM surface morphology of a nanowire film after annealing at 300 °C for 1 h displaying a clear cracking pattern consistent with a contraction of structure upon conversion to ZnO.

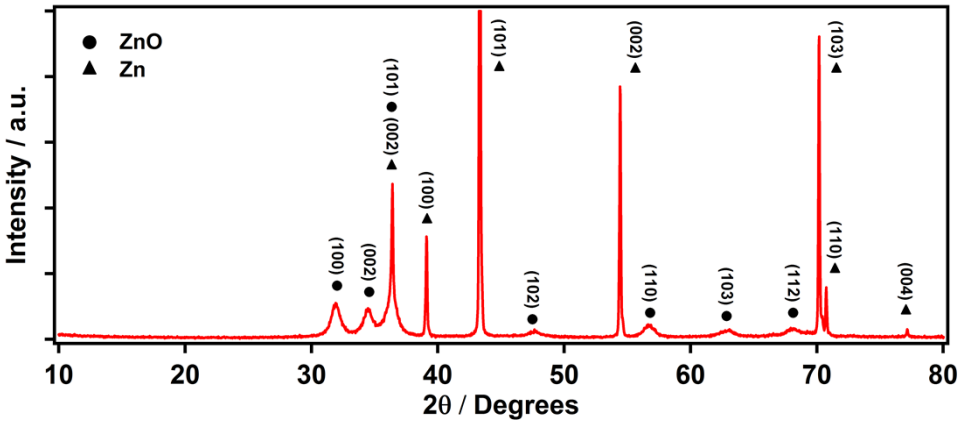

Figure S11. Flat plate XRD pattern of the hierarchical ZnO nanowires formed from treating the anodic ZnO nanowires in water.

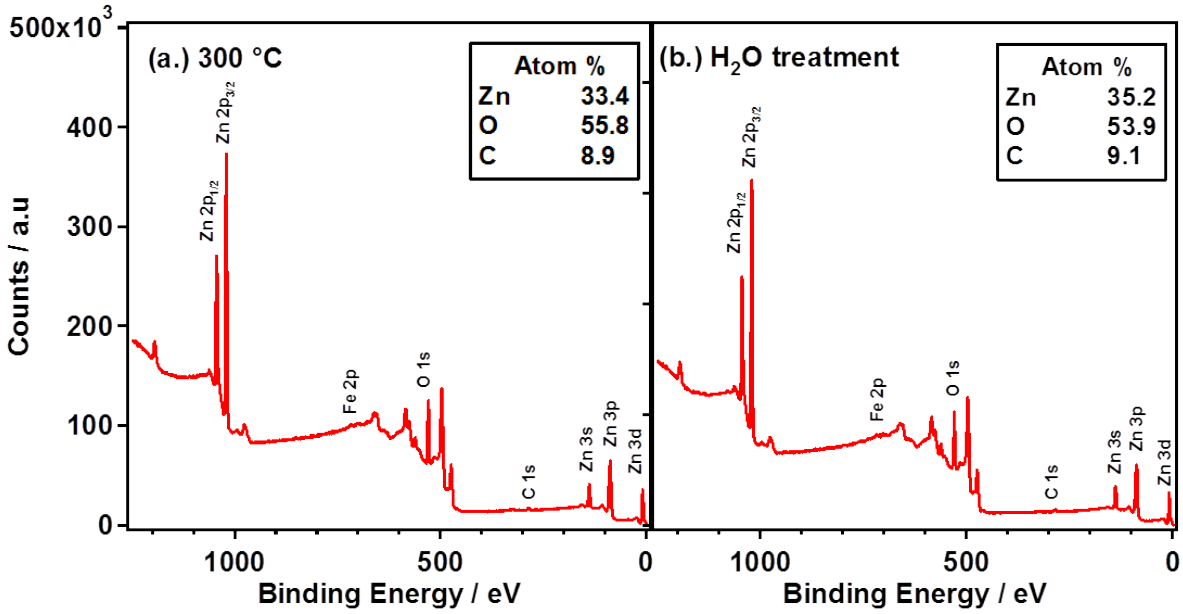

Figure S12. X-ray photoelectron spectrum of the polycrystalline ZnO nanowires with a slit-type pore structure (a) and with a hierarchical structure after water treatment (b).